Surface water chemistry and nitrate pollution in Shimabara, Nagasaki, Japan

Hiroki Amano・Kei Nakagawa・Ronny Berndtsson

H. Amano・K. Nakagawa (✉)*

Graduate School of Fisheries and Environmental Sciences, Nagasaki University,

1-14 Bunkyo-machi, Nagasaki 852-8521, Japan

* Corresponding author

e-mail: kei-naka@nagasaki-u.ac.jp

Tel.: +81 95 819 2763; fax: +81 95 819 2763

R. Berndtsson

Division of Water Resources Engineering & Center for Middle Eastern Studies, Lund University, Box 118, SE-221 00 Lund, Sweden

Abstract

Groundwater is a finite resource that is threatened by pollution all over the world. Shimabara City, Nagasaki, Japan, uses groundwater for its main water supply. During recent years, the city has experienced severe nitrate pollution in its groundwater. For better understanding of origin and impact of the pollution, chemical effects and surface-groundwater interactions need to be examined. For this purpose, we developed a methodology that builds on joint geochemical analyses and advanced statistical treatment. Water samples were collected at 42 sampling points in Shimabara including a part of Unzen City. Spatial distribution of water chemistry constituents was assessed by describing hexa and trilinear diagrams using major ions concentrations. The nitrate (NO_3+NO_2-N) concentration in 45% of water samples exceeded permissible Japanese drinking level of 10 mg L^{-1}. Most of the samples showed Ca-HCO_3 or Ca-(NO_3+SO_4) water types. Some samples were classified into characteristic water types such as Na-Cl, (Na+K)-HCO_3, (Na+K)-(SO_4+NO_3), and Ca-Cl. Thus, results indicated salt water intrusion from the sea and anthropogenic pollution. At the upstream of Nishi River, although water chemistry was characterized as Ca-HCO_3, ion concentrations were higher than those of other rivers. This is probably an effect of disinfection in livestock farming using slaked lime. Positive correlation between NO_3^- and SO_4^{2-}, Mg^{2+}, Ca^{2+}, Na^+, K^+, and Cl^- (r = 0.32 - 0.64) is evidence that nitrate pollution sources are chemical fertilizers and livestock waste. Principal component analyses showed that chemistry of water samples can be explained by three main components (PCs). PC1

depicts general ion concentration. PC2 and PC3 share influence from chemical fertilizer and livestock waste. Cluster analyses grouped water samples into four main clusters. One of these is the general river chemistry mainly affected by PC1. The others reflect anthropogenic activities, and are identified by the combination of the three PCs.

Key words: Surface water, Water chemistry, Nitrate pollution, Correlation analysis, Principal component analysis, Hierarchical cluster analysis

Introduction

Shimabara City, Nagasaki, Japan, has experienced serious nitrate pollution of groundwater. Groundwater is commonly used for public water supply in the area. For this reason, Nakagawa et al. (2016) investigated water chemistry and nitrate pollution in the groundwater. They found that unaffected groundwater could be classified as Ca-HCO_3 while nitrate polluted groundwater was classified as Ca-(SO_4+NO_3). Nitrate concentration was found to exceed Japanese drinking standard (10 mg L^{-1}) at 15 of 40 locations. The results indicated that NO_3^- pollution in the area is related to livestock waste, chemical fertilizer, and calcareous material to neutralize acid soil. Principal component analysis showed that the water chemistry is characterized by ion dissolution during groundwater flow and nitrate pollution sources. Other nearby areas, such as the Nishi River, has as

well been confirmed to be polluted by nitrate. A typical denominator for the polluted areas is that they are drained by small rivers flowing from the mountainside to the seashore. For a better understanding of the nature of the nitrate pollutant source, geochemistry, and surface and groundwater interactions need to be better understood (Vrzel et al., 2018).

Surface water chemistry is affected by various biogeochemical processes (especially atmospheric precipitation, chemical weathering, and evapo-crystallization) and anthropogenic factors (Pant et al., 2018). Many researchers have investigated river water chemistry and controlling factors by different approaches such as; water quality index (WQI) (Kannel et al., 2007; Şener et al., 2017), principal component analysis (PCA) (Ouyang, 2005; Lee et al., 2017), factor analysis (Mir et al., 2016), geographic information system (GIS) (Şener et al., 2017), and temporal sampling (Sun et al., 2010; Mir et al., 2016). In recent years, pollution and degradation of surface water have been shown to cause environmental and potential social problems and risks to public health (Le et al., 2017). Human factors such as agriculture (fertilizers and agrochemical methods, irrigation, and livestock operation), industry, and wastewater have caused pollution by bacteria and virus, fecal sterols, and chemicals like inorganic ions, and trace and toxic metals for rivers in many countries (Bulut et al., 2010; Obiri-Danso et al., 2011; Chigor et al., 2012; Furtula et al., 2012; Li et al., 2014; Olkowska et al., 2014; Wilbers et al., 2014). These pollutants increasingly result in water chemical levels exceeding World Health Organization (WHO) guidelines.

In this study, we present a methodology that can be used to investigate nitrate pollution sources for the groundwater. The methodology builds on geochemical sampling together with advanced statistical treatment. The results can be used to estimate the relative contribution of different pollution sources to groundwater, impact on water quality, and management to improve the polluted sites. A first step for assessing influence from surface water to groundwater, is the spatial distribution of water chemistry, nitrate pollution, and surface water forming factors using graphical methods (Stiff and Piper diagrams). Secondly, multivariate analyses (principal components analysis and hierarchical cluster analysis) are used in combination with the sampled data.

Materials and methods

Study area

Figure 1 shows the location of Shimabara City and sampling sites. Shimabara City is one of the districts forming Shimabara Peninsula. The city covers 82.8 km^2, which constitute about 18% of the peninsula. The geology of Shimabara is formed by volcanic activities, resulting in volcanic rocks over-laying marine and non-marine deposits (Fig. 2; Geological Survey of Japan, 2017). The city area is constituted by three main types of land use; forest, upland fields, and urban areas (Fig. 2). The upland fields are important for supplying vegetables (mainly Chinese radish and cabbage and carrot). On the mountain side of the upland fields, livestock facilities are located. Livestock numbers

correspond to about 1,000 milk cattle, 22,900 pigs, and 1,028,200 hens (2015). Most of the livestock production are located in the upstream areas of the Nishi and Yue Rivers. Average annual temperature was 17.1℃ in 2017. The average monthly temperature ranges from 7.0 to 18.9℃. Annual rainfall was 1,989 mm in 2017.

Water sampling and chemical analyses

The suggested methodology to investigate groundwater pollution sources in Shimabara involved water sampling with chemical analyses and advanced statistical analyses according to the below. Water samples were collected at 42 sampling sites from 15 rivers in Shimabara including a region of Unzen City on January 17 and 24, as well as on February 6 in 2017. In Yue and Nishi River, more sampling points were chosen to understand the transition of water chemistry from upstream to downstream. Water samples were collected directly from the center sections of the rivers in pre-washed bottles except for sampling sites 6 and 27. Physicochemical parameters such as pH, electrical conductivity (EC), oxidation redox potential (ORP), dissolved oxygen (DO), temperature, and HCO_3^- were determined in-situ. Portable meters (HORIBA D-51, and 54) were used for pH, EC, and ORP. DO and temperature were measured using a luminescence-based sensor (HACH HQ30d). HCO_3^- was quantified using titration method with 0.1 N HCl. Major dissolved anions (Cl^-, NO_2^-, NO_3^-, and SO_4^{2-}) and cations (Na^+, NH_4^+, K^+, Mg^{2+}, and Ca^{2+}) were analyzed with ion chromatography (Metrohm 861

Advanced Compact IC).

Multivariate analyses

Multivariate analyses based on water chemistry data can be used to improve the understanding of relationships, source of ions, and factors regulating water chemistry. In this study, correlation analysis, principal component analysis (PCA), and hierarchal cluster analysis (HCA) were performed using all ion concentrations except for site 15 where river water is mixed with sea water. Multivariate analyses were performed using the statistical software JMP Pro 13 (SAS Institute Inc.). NO_2^- and NH_4^+ were not detected in a number of samples. The LOD (limit of detection 0.135 and 0.21 mg L^{-1}, respectively) values were used in the multivariate analysis for these samples.

Results and discussion

General surface water chemistry

Measured hydrochemical parameters for each site are presented in Table 1. Temperature of the surface water ranged from 4.2 to 17.2°C. It reflects the atmospheric temperature during the sampling campaign (1.2-10.9°C). The pH showed a small range with weak acidic conditions. The ORP was positive, ranging from 147 to 280 mV except for sites 19 and 27. Significantly small values (26.5 and 28.1 mV, respectively) were observed at these sites. The DO ranged from 7.8 to 11.6 mg L^{-1} except

for sites 30, 31, and 32 with notably small values from 0.70 to 2.48. These sites are located in the upstream areas of Nishi River, where ammonium (NH_4^+), nitrite (NO_2^-), and nitrate (NO_3^-) were detected. Due to small DO this may result in small nitrification.

Water chemistry patterns were assessed using Stiff and Piper diagrams based on major ion concentration data. Figure 3 shows the Piper diagram for the 42 surface water samples. Most of the samples are located in Class I or Class III. Class I is dominated by calcium and bicarbonate, corresponding to the common major element composition of the surface water. The water samples from the Unzen River (site 17 to 20), the southern parts of Shimabara (site 1 to 8, 28, and 29), the midstream of Nishi River (site 27 and 30), and the upstream of Yue River (site 33), are included in this class. Water samples dominated by calcium, nitrate, and sulfate are located in Class III. In case of groundwater, nitrate polluted samples are found in Class III (Nakagawa et al., 2016). Thus, this class indicates nitrate polluted surface water. Most of the samples from the northern parts of Shimabara (site 9 to 14, 16, 21 to 26, and 34 to 42) fall within this class. As shown Table 1, all these sampling sited displayed high nitrate concentrations (>37.5 mg L^{-1}). Two water samples are located in Class IV, commonly indicating sea water mixing with respect to sodium and chloride. One of the samples (site 15) is from the far downstream of Yue River close to the coastline. According to Chester and Jickells (2012), sodium and chloride are principal dissolved components of sea water. The other sample was collected from the upstream of Nishi River (site 31). This site is located on the mountainside (Fig. 1),

not being exposed to sea water. Anthropogenic pollutants are probably important sources for Na^+, K^+, and NO_3^- at this site. Only one sample (site 32) was located in Class II related to sodium, potassium, and bicarbonate. As mentioned above, NH_4^+ and NO_2^- were found at site 31 and 32. These pollutants likely come from livestock waste from farms located close to the river.

Figure 4 shows the spatial distribution of water chemistry using Stiff diagrams for the 42 sampling sites. Most of the samples display Ca-HCO_3 or Ca-(SO_4+NO_3) water types. Several samples are characterized as Na-Cl, (Na+K)-HCO_3, (Na+K)-(SO_4+NO_3), and Ca-Cl. This indicates mixing with seawater together with anthropogenic pollution. The spatial characteristics of surface water represented by the Stiff diagrams are similar to those of the groundwater (Nakagawa et al., 2016), indicating surface water-groundwater mixing. With river flow from upstream to downstream in the Yue River, water types transit from Ca-HCO_3 to Ca-(SO_4+NO_3), and further to Na-Cl due to sea water mixing, and general ion concentrations in the mainstream tend to increase at the lower site 22 and 23. Tributaries, with high ion concentrations, join the main river upstream these sites, resulting in significant increase in ion concentration. (Na+K)-HCO_3 type water is transformed to Ca-HCO_3 and eventually to Ca-(SO_4+NO_3) along the river flow in Nishi River. The chemical composition drastically changed and decreased between site 27 and site 10 because of significant contribution of groundwater inflow. The water chemistry in the lower reaches of the river at site 9 and 10 is essentially the same as for groundwater collected close to these sites. Although, Ca-HCO_3 types were confirmed at the

upstream of the Nishi River, the concentration of ions is higher than in the groundwater in this region.

For disinfection purposes, livestock farms use slaked lime (calcium hydroxide). After use, the lime is usually washed out to the rivers by rain. This means that the Ca^{2+} concentration will increase in the downstream. NO_3^- originating from livestock waste will likely be exposed to denitrification. This means that NO_3^- will decrease and HCO_3^- increase according to:

$$5C + 4NO_3^- + H_2O \rightarrow 2N_2 + 4HCO_3^- + CO_2$$

According to this relationship, livestock waste together with slaked lime will lead to high concentration of Ca-HCO_3 as can be noticed at sites 27 and 30.

Nitrate (NO_3+NO_2-N) pollution

Spatial dstribution of nitrate (NO_3+NO_2-N) concentrations are shown in Fig. 5. NO_2-N was detected at two sampling sites 30 and 32 upstream of Nishi River. The concentration exceeded the drinking standard of 0.9 mg L^{-1} for bottle-fed infants (WHO, 2011). The nitrate concentration ranged from 1.0 to 27.5 mg L^{-1} with an average of 9.7 mg L^{-1}. The highest concentration (27.5 mg L^{-1}) was found at site 31. The nitrate concentrations exceeded the Japanese drinking water standards of 10 mg L^{-1} at 19 sampling sites. Relatively high concentrations of nitrate were observed in the rivers coming from the northern parts of the study area containing the upland fields.

Multivariate analysis

Correlation analysis

Correlation analysis was performed for all measured ions concentrations (Cl^-, NO_2^-, NO_3^-, SO_4^{2-}, HCO_3^-, Na^+, NH_4^+, K^+, Mg^{2+}, and Ca^{2+}) except for site 15 because ion concentrations here were much larger due to sea water mixing. Table 2 shows results of the correlation analysis using 41 sampling sites. Unzen volcanic rocks distributed in Shimabara are composed of hornblende andesite to dacite, which has a phenocryst of plagioclase, hornblende, and biotite (Sugimoto, 2006). The correlation in Table 2 follows naturally occurring geochemical processes: (1) The strong positive correlation between Na^+ - HCO_3^- and K^+ - HCO_3^- (r = 0.74 and 0.76, respectively) imply weathering of plagioclase (albite and K-feldspar). The chemical reaction can be expressed as (Sun et al., 2017):

$$2NaAlSi_3O_8 + 2CO_2 + 11H_2O \rightarrow Al_2Si_2O_5(OH)_4 + 2HCO_3^- + 2Na^+ + H_4SiO_4$$

$$2KAlSi_3O_8 + 2CO_2 + 6\,H_2O \rightarrow Al_2Si_4O_{10}(OH)_2 + 2HCO_3^- + 2K^+ + 2H_4SiO_4$$

(2) Ca^{2+} is moderately correlated with HCO_3^- (r = 0.40), indicating weathering of plagioclase (anorthite) according to:

$$CaAl_2Si_2O_8 + 2CO_2 + 3H_2O \rightarrow Al_2Si_2O_5(OH)_4 + 2HCO_3^- + Ca^{2+}$$

(3) The strong positive correlation between Na^+, Mg^{2+}, and Ca^{2+} (r = 0.59 – 0.80), implies weathering of hornblende that is expressed in the stoichiometric dissolution (Velbel, 1989):

$$Na_{0.5}Ca_2(Fe_{1.3}Mg_{2.6}Al_{1.1})(Al_{1.6}Si_{6.4})O_{22}(OH)_2 + 15H^+ + H_2O \rightarrow 0.5Na^+ + 2Ca^{2+} + 2Mg^{2+} +$$

$1.3Fe^{2+} + 2.7Al(OH)_2^{+} + 6.4H_4SiO_4$

Some of the observed correlation can be interpreted as effects of anthropogenic influence: (1) Positive correlation between SO_4^{2-}, NO_3^-, Mg^{2+}, and Ca^{2+} indicates influence from a common origin that likely is chemical fertilizers (Babiker et al., 2004). The correlation among these ions was r = 0.37-0.80. Ammonium sulfate ($(NH_4)_2SO_4$) is commonly applied together with slaked lime and magnesia lime ($(Ca, Mg)CO_3$) as fertilizer in this area (Nakagawa et al., 2016). No correlation was found between NH_4^+ and SO_4^{2+}, which is consequence of nitrification changing NH_4^+ to NO_3^-. (2) Strong and moderate positive correlation between Na^+, K^+, Cl^-, and SO_4^{2-} indicates their common origin, and can be explained in terms of influence of pig farm wastewater (Fridrich et al., 2014). Cl^- is a predominant anion in manure from livestock waste (Oyanagi, 2004). NH_4^+ is often positively correlated with K^+ and Cl^- in groundwater under pig farming (Fridrich et al., 2014). Similar results were found in this study. There was a strong and positive correlation between Na^+, K^+, and Cl^- (r = 0.74 - 0.81). NH_4^+ was positively correlated with Cl^- and K^+. There are pig farms along the upstream of Nishi River close to site 32. Although the nitrogen supply from households is only one tenth of nitrogen supply from the farm animal sector, considering that the domestic wastewater treatment coverage is only 52.4% (2014), domestic wastewater is a possible source for Cl^-.

In view of the above, Cl^-, NO_3^-, SO_4^{2-}, and NH_4^+ can be seen as originating from anthropogenic activities. Although, Na^+, K^+, Mg^{2+}, and Ca^{2+} generally can be regarded as having

natural origin in non-polluted water, these cations are likely to be enhanced by anthropogenic activities as observed polluted water. As shown in Fig. 4, polluted water samples tend to have higher concentrations of these ions as compared to non-polluted samples.

Principal component analysis (PCA)

The ten hydrochemical variables (Cl^-, NO_2^-, NO_3^-, SO_4^{2-}, HCO_3^-, Na^+, NH_4^+, K^+, Mg^{2+}, and Ca^{2+}) were used as input to the PCA analysis. The input data were standardized before analysis. PCA was applied using the correlation matrix between chemical elements. Figure 6 shows the relationship between obtained PCs and investigated ions. In accordance with the Kiser criteria, only principal components (PC) with eigenvalue greater than 1.0 was kept for further analyses. Thus, three PCs were extracted. The eigenvalues for these PCs ranged from 1.09 to 5.38, explaining 88.3% of the total variance.

PC1, accounting for 53.8% of the total variance, had positive loadings for all ions, which indicate that this component is related to the mean ion concentration. PC2 was characterized by positive loadings for SO_4^{2-}, NO_3^-, Mg^{2+}, and Ca^{2+}, and negative loadings for HCO_3^-, NH_4^+, NO_2^-, and K^+. It explained 23.6% of the total variance. The positive relationship among SO_4^{2-}, NO_3^-, Mg^{2+}, and Ca^{2+} indicates a similar origin (chemical fertilizer) as mentioned above. The relationship between NO_3^-, NH_4^+, and NO_2^- represents the nitrification process from NH_4^+ ($NH_4^+ \rightarrow NO_2^- \rightarrow NO_3^-$) originating

from the chemical fertilizer NH_4SO_4. Negative HCO_3^- can be explained by the fact that nitrification decreases the HCO_3^- concentration. In contrast to the use of chemical fertilizers, the association between NH_4^+, NO_2^-, and K^+ implies influence of livestock effluents. Thus, PC2 helps to identify the pollution source. PC3 is, however, also interpreted as a result from livestock effluents due to joint positive loading of NO_3^-, NH_4^+, and K^+. It accounts for 10.9% of the total variance.

Hierarchical cluster analysis (HCA)

HCA was performed based on the three PC scores outlined above (see also Amano et al., 2016a). The classification result of each sample is represented in the dendrogram shown in Fig. 7. In total 41 water samples were classified into four distinct groups. Samples of Groups 3 and 4 were combined with the other groups in the final linkage step, indicating that the water chemistry of these samples are least similar to that of other groups. Significant dissimilarity between Group 1 and 2 is expected because the linkage distance between these is at a maximum. Group 3, as well, is dissimilar to Group 4 due to large linkage distance. Table 3 shows the average ion concentration of each group as representing the water characteristics. Group 1 is related to HCO_3^- for anions and Ca^{2+} for cations, which is a normal major element composition for surface waters. Group 2 is recognized as a nitrate polluted group due to high nitrate concentrations. NO_2^- and NH_4^+ are classified in Group 3. The NO_2^- concentration is above the drinking water standard of 0.9 mg L^{-1} as regards NO_2-N. If all ions are

converted to NO_3^-, a total of 82.7 mg L^{-1} of NO_3^- would result. Thus, although this group still satisfy the drinking water standard for NO_3^- (WHO, 2011), it could potentially exceed the drinking water standard. Group 4, in which only one water sample was classified, generally showed large ion concentrations. In particular, Cl^-, NO_3^-, K^+, and NH_4^+ concentrations were larger than for any other group, indicating pollution by livestock wastewater.

Figure 8 shows the relationship between the three PCs for the 41 water samples classified into four groups. PC1, namely mean ion concentration, apparently separates Group 3 and 4 from Group 1 and 2. Smaller PC1 scores explain that Group 1 has less ion concentration compared to Group 3 and 4. It can, thus, be confirmed that Group 1 has low ion concentrations and represents a non-polluted group. Group 2 displays higher PC1 scores as compared to Group 1. In addition, Group 2 is easily distinguishable due to positive PC2 scores as compared to the other groups. Positive PC2 is interpreted as influenced by chemical fertilizer, indicating that it has higher ion concentration than Group 1. Although Group 3 and 4 show similar PC scores for PC1 and 2, they are distinguished by PC3 (Fig.8). Both groups have negative PC2 scores, which shows the effect of livestock effluents. Positive PC1 and negative PC2 scores explain that Group 3 and 4 are polluted by livestock wastes. Positive PC3 scores reveal that Group 4 is significantly more influenced by livestock effluents as compared to Group 3 as seen in Table 3.

As shown in Fig. 9, distinct spatial distributions for each group can be observed. Samples in

Group 1 were generally observed in the southern part in urban areas. A part of these are found in the upstream of the Yue River (33, 34, and 36) and Rivers of Unzen City (17, 18, 19, and 20). These sampling locations are situated in the forest and urban areas (Fig. 2). Sample 33 has small ion concentration because the site is located in the most upstream part of the river and influence of agricultural activities is small. As well, samples 34 and 36 had less ion concentration compared to the downstream and tributaries. Although nitrate concentration was below Japanese drinking water standard, total concentration may be elevated due to agricultural activities. It is noted that Group 2, which is distinguishable with positive PC2 scores (chemical fertilizer), is distributed in the upstream areas. There results concur with previous studies (Nakagawa et al., 2016). A few samples that were classified into Group 3 and 4 are located only in the upstream of the Yue River. Consequently, samples collected in the northern and southern rivers flowing a short distance and urban areas close to the mountain, did not present nitrate pollution. On the other hand, Yue and Nishi River, passing through the dense upland area with livestock farming, were seriously polluted by nitrate except for the three specific samples from the upstream of Yue River.

Conclusions

This study presented a methodology to investigate hydrogeochemical characteristics and nitrate pollution of surface water and influencing factors. Besides water sampling and chemical

analyses, the methodology involved the use of Piper and Stiff diagrams and multivariate statistical analyses. The study revealed mineral dissolution as well as effects of anthropogenic activities on surface water chemistry. The surface water was in general weakly acidic and oxidizing conditions were shown by pH, DO, and ORP. Piper and Stiff diagrams indicated that the dominant water types are Ca-HCO_3 and Ca-(SO_4+NO_3), which is consistent with groundwater chemistry in the area. Local sea water and anthropogenic activities resulted in some minor water types such as Na-Cl, (Na+K)-HCO_3, (Na+K)-(SO_4+NO_3), and Ca-Cl. Correlation analyses indicated that weathering of gypsum, anhydrite, and silicate minerals are the dominant sources of ions. Chemical fertilizers and livestock waste influence surface water chemistry and cause severe nitrate pollution especially in the northern parts of the city. The nitrate contaminated samples above Japanese standard drinking water levels occupied 45% of all samples. PCA extracted three significant PCs explaining 88.3% of total variance. This reflects mean ion concentrations, and effects of chemical fertilizers and livestock effluents. Based on the PCA results, four distinct water groups were obtained by HCA. The chemical composition of these groups was different in terms of land use, and importance of the three PC scores. In general, the spatial distribution of surface water chemistry was similar to that of the groundwater, implying strong interaction between surface and groundwater. Although, Shimabara City only uses groundwater for public water use, quantifying the influence of surface water on groundwater is required for resolving the nitrate pollution problem.

Acknowledgements

This work was supported by JSPS KAKENHI Grant Number JP15KT0120 and JP16KK0014.

References

Amano, H., Nakagawa, K., Kawamura, A. (2016a) Classification characteristics of multivariate analyses for groundwater chemistry - case study of Shimabara City -. Journal of Japan Society of Civil Engineers, Ser. G (Environmental Research) 71(6): I_127-I_135 (in Japanese with English abstract).

Amano, H., Nakagawa, K., Berndtsson, R. (2016b) Groundwater geochemistry of a nitrate-contaminated agricultural site. Environmental Earth Sciences 75: 1145.

Babiker, I. S., Mohamed, M. A. A., Terao, H., Kato, K., Ohta, K. (2004) Assessment of groundwater contamination by nitrate leaching from intensive vegetable cultivation using geographical information system. Environment International 29: 1009-1007.

Bulut, V.N., Bayram, A., Gundogdu, A., Soylak, M., Tufekci, M. (2010) Assessment of water quality parameters in the stream Galyan, Trabzon, Turkey. Environmental Monitoring and Assessment 165(1-4): 1-13.

Chester, R and Jickells, T. D. (2012) Marine Geochemistry, Third Edition. Wiley Blackwell, London,

420pp.

Chigor, V. N., Umoh, V. J., Okuofu, C. A., Ameh, J. B., Igbinosa, E. O., Okoh, A. I. (2012) Water quality assessment: Surface water sources used for drinking and irrigation in Zaria, Nigeria are a public health hazard. Environmental Monitoring and Assessment 184(5): 3389-3400.

Committee on Nitrate Reduction in Shimabara Peninsula (2016) The second term of Shimabara Peninsula nitrate load reduction project, revised edn., Environmental Policy Division of Nagasaki Prefectural Government, Nagasaki. http://www.pref.nagasaki.jp/shared/uploads/03/1459226718.pdf. Accessed 23 Feb 2018 (in Japanese).

Dalai, T. K., Krishnaswami, S., Sarin, M. M. (2002) Major ion chemistry in the headwaters of the Yamuna River system: chemical weathering, its temperature dependence and CO_2 consumption in the Himalaya. Geochimica et Cosmochimica Acta 66(19): 3397–3416.

Fridrich, B., Krčmar, D., Dalmacija, B., Molnar, J., Pešić, V., Kragulj, M., Varga, N. (2014) Impact of wastewater from pig farm lagoons on the quality of local groundwater. Agricultural Water Management 135: 40-53.

Fujii, H., Nakagawa, K., Kagabu, M. (2016) Decomposition approach of nitrogen generation process: empirical study on the Shimabara Peninsula in Japan. Environmental Science and Pollution Research 23(22): 23249-23261.

Furtula, V., Osachoff, H., Derksen, G., Juahir, H., Colodey, A., Chambers, P. (2012) Inorganic nitrogen,

sterols and bacterial source tracking as tools to characterize water quality and possible contamination sources in surface water. Water Research 46(4): 1079-1092.

Geological Survey of Japan (2017) Seamless Digital Geological Map of Japan (1:200,000), https://gbank.gsj.jp/seamless/ (accessed May 29 2017).

Kannel, P. R., Lee, S., Lee, Y. S. (2007) Application of Water Quality Indices and Dissolved Oxygen as Indicators for River Water Classification and Urban Impact Assessment. Environmental Monitoring and Assessment 132(1-3): 93-110.

Lee, T. T. H., Zeunert, S., Lorenz, M. (2017) Multivariate statistical assessment of a polluted river under nitrification inhibition in the tropics. Environmental Science and Pollution Research 24(15): 13845-13862.

Li, J., Li, F., Liu, Q., Song, S., Zhang, Y., Zhao, G. (2014) Impacts of Yellow River Irrigation Practices on Trace Metals in Surface Water: A case study of the Henan-Liaocheng Irrigation Area, China. Human and Ecological Risk Assessment 20(4): 1042-1057.

Mir, R. A., Jeelani, G., Dar, F. A. (2016) Spatio-temporal patterns and factors controlling the hydrogeochemistry of river Jhelum basin, Kashmir Himalaya. Environmental Monitoring and Assessment 188: 438.

Nakagawa, K., Amano, H., Asakura, H., Berndtsson, R. (2016) Spatial trends of nitrate pollution and groundwater chemistry in Shimabara, Nagasaki, Japan. Environmental Earth Sciences 75(3):

234.

Obiri-Danso, K., Adonadaga, M. G., Hogarh, J. N. (2011) Effect of agrochemical use on the drinking water quality of Agogo, a tomato growing community in Ashanti Akim, Ghana. Bulletin of Environmental Contamination and Toxicology 86(1): 71-77.

Olkowska, E., Kudłak, B., Tsakovski, S., Ruman, M., Simeonov, V., Polkowska, Z. (2014) Assessment of the water quality of Kłodnica River catchment using self-organizing maps. Science of the Total Environment 476-477: 477-484.

Ouyang, Y. (2005) Evaluation of river water quality monitoring stations by principal component analysis. Water Research 39: 2621-2635.

Oyanagi, W., Ando, Y., Mizusawa, S, Moriyama, N. (2004) Salt composition characteristics of animal waste composts. Society of Soil Science and Plant Nutrition 75(1): 91-93.

Pant, R. R., Zhang, F., Rehman, F. U., Wang, G., Ye, M., Zeng, C., Tang, H. (2018) Spatiotemporal variations of hydrochemistry and its controlling factors in the Gandaki River Basin, Central Himalaya Nepal. Science of the Total Environment 622-623: 770-782.

Şener, Ş., Şener, E., Davraz, A. (2017) Evaluation of water quality using water quality index (WQI) method and GIS in Aksu River (SW-Turkey). Science of the Total Environment 584-585: 131-144.

Sugimoto, T. (2006) Geology and petrology at Shimabara Peninsula, Kyushu, SW Japan –From recent

results-. Journal of the Geothermal Research Society of Japan 28(4): 347-360.

Skórczewski, P., Mudryk, Z. (2009) Bacterial pollution of the riverine surface microlayer and subsurface water. Water Science and Technology 60(1): 127-134.

Sun, X., Mörth, C. M., Humborg, C., Gustafsson, B. (2017) Temporal and spatial variations of rock weathering and CO_2 consumption in the Baltic Sea catchment. Chemical Geology 466(5): 57-69.

Sun, H., Han, J., Li, D., Zhang, S., Lu, X. (2010) Chemical weathering inferred from riverine water chemistry in the lower Xijiang basin, South China. Science of the Total Environment 408: 4749-4760.

Velbel, M. A. (1989) Weathering of hornblende to ferruginous by a dissolution-reprecipitation mechanism: Petrography and stoichiometry. Clays and Clay Minerals 37(6): 515-524.

Vrzel, J., Solomon, D. K., Blažeka, Z., Ogrinc, N. (2018) The study of the interactions between groundwater and Sava River water in the Ljubljansko polje aquifer system (Slovenia). Journal of Hydrology 556: 384-396.

Wilbers, G.-J., Becker, M., Nga, L. T., Sebesvari, Z., Renaud, F. G. (2014) Spatial and temporal variability of surface water pollution in the Mekong Delta, Vietnam. Science of the Total Environment 485-486: 653-665.

WHO (World Health Organization) (2011) Guidelines for drinking water quality, 4th edn. WHO Press,

Geneva

Figure captions

Fig. 1 Location map of study area and sampling sites

Fig. 2 Geology and land use map

Fig. 3 Piper diagram for surface water samples

Fig. 4 Spatial distribution of water chemistry with Stiff diagram

Fig. 5 Spatial distribution of nitrate (NO_3+NO_2-N) concentration

Fig. 6 Relationship between extracted three PCs and ions

Fig. 7 Dendrogram for grouped surface water samples with site identification

Fig. 8 Scatter diagram showing relationship between three PCs

Fig. 9 Distribution of each group in the study area

Table captions

Table 1 Summary of measured hydrochemical parameters

Table 2 Correlation matrix between dissolved ions

Table 3 Average dissolved ion concentrations for each group

Figure 1

Click here to download Figure Fig 1.tif

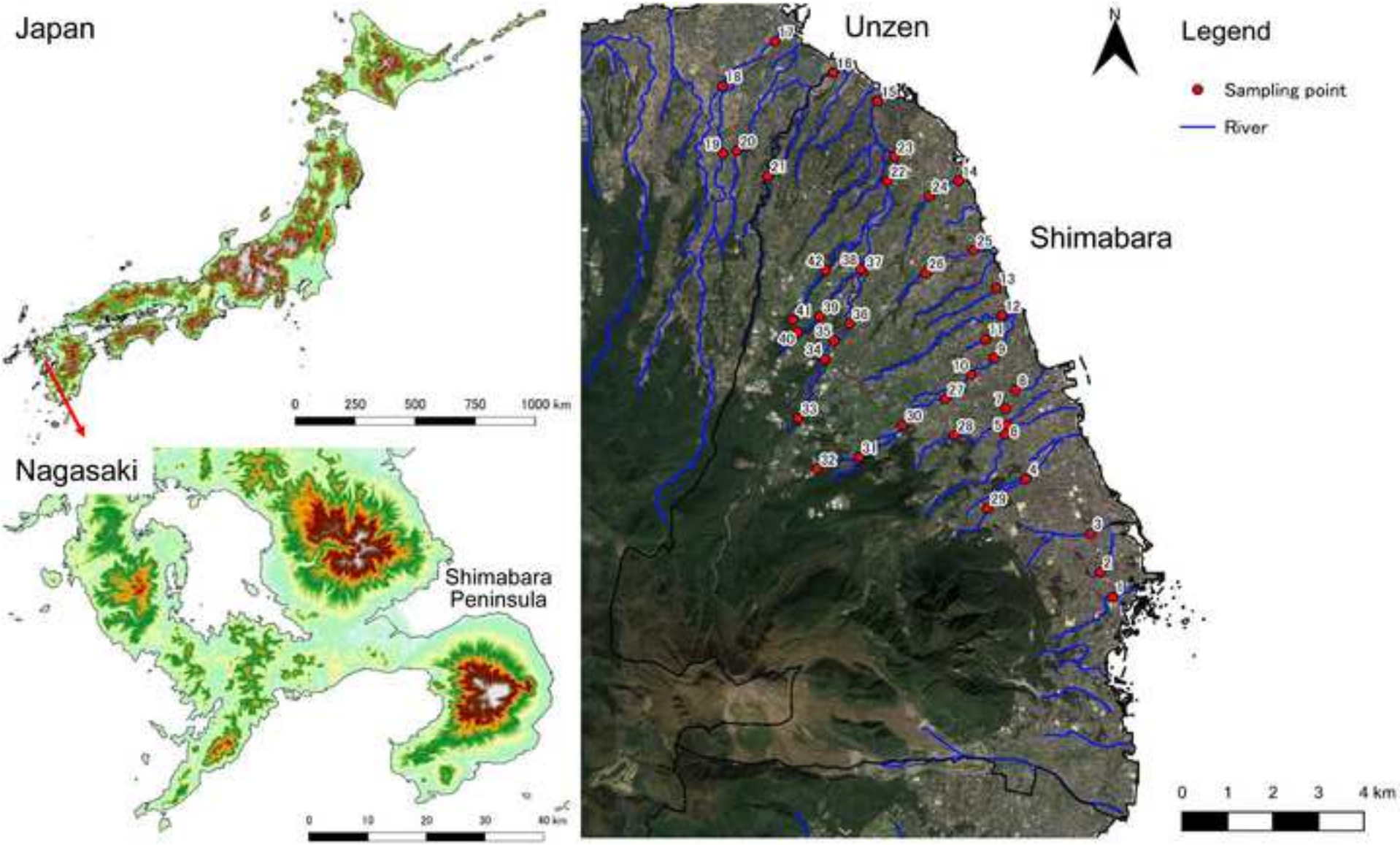

Figure 2

Click here to download Figure Fig 2.tif

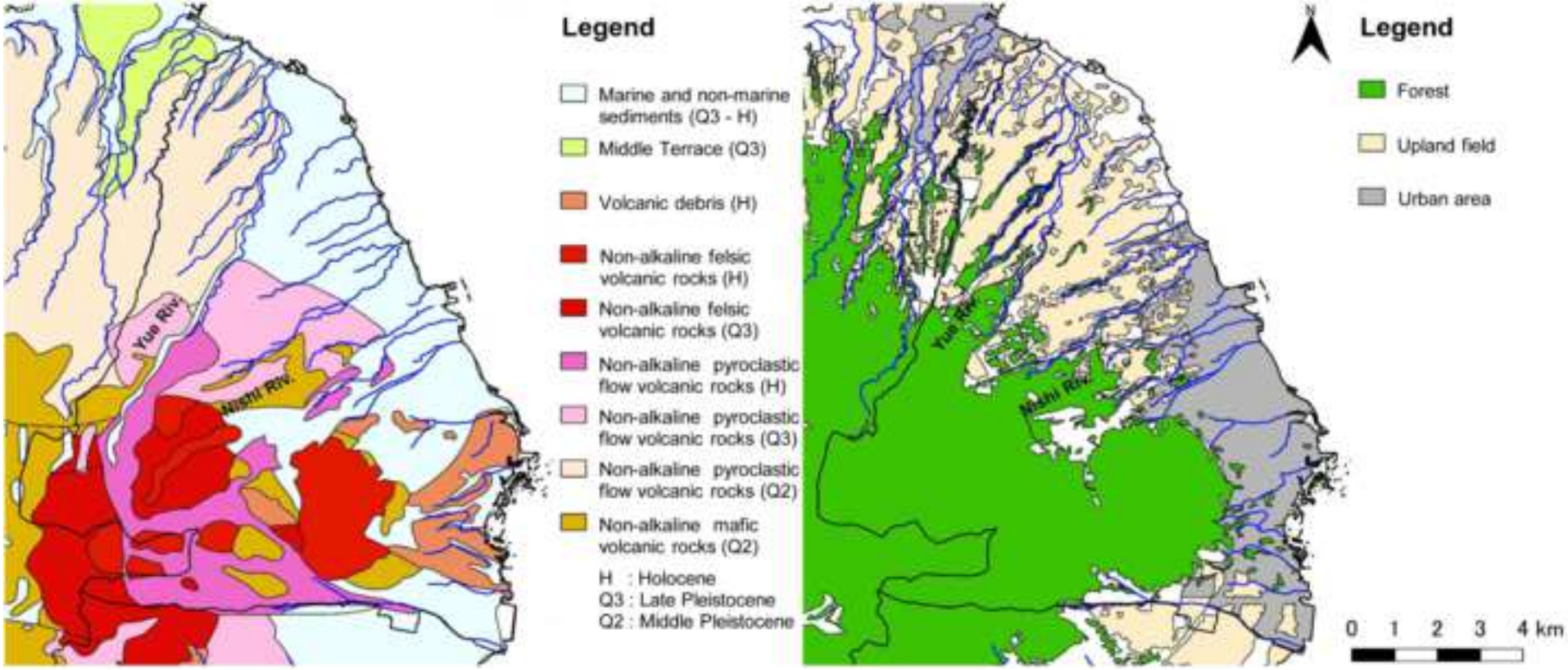

Figure 3

Click here to download Figure Fig 3.tif

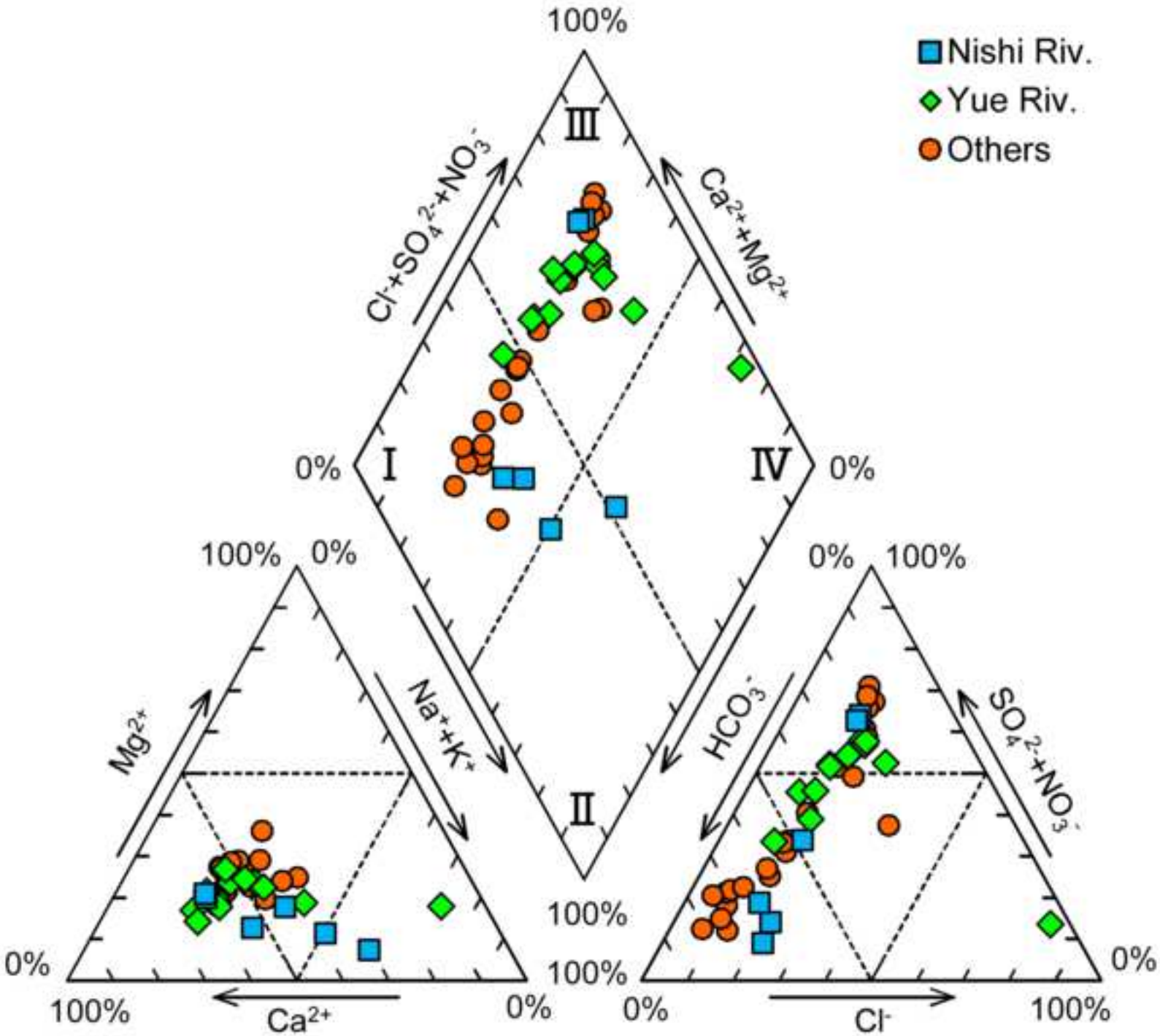

Figure 4

Click here to download Figure Fig 4.tif

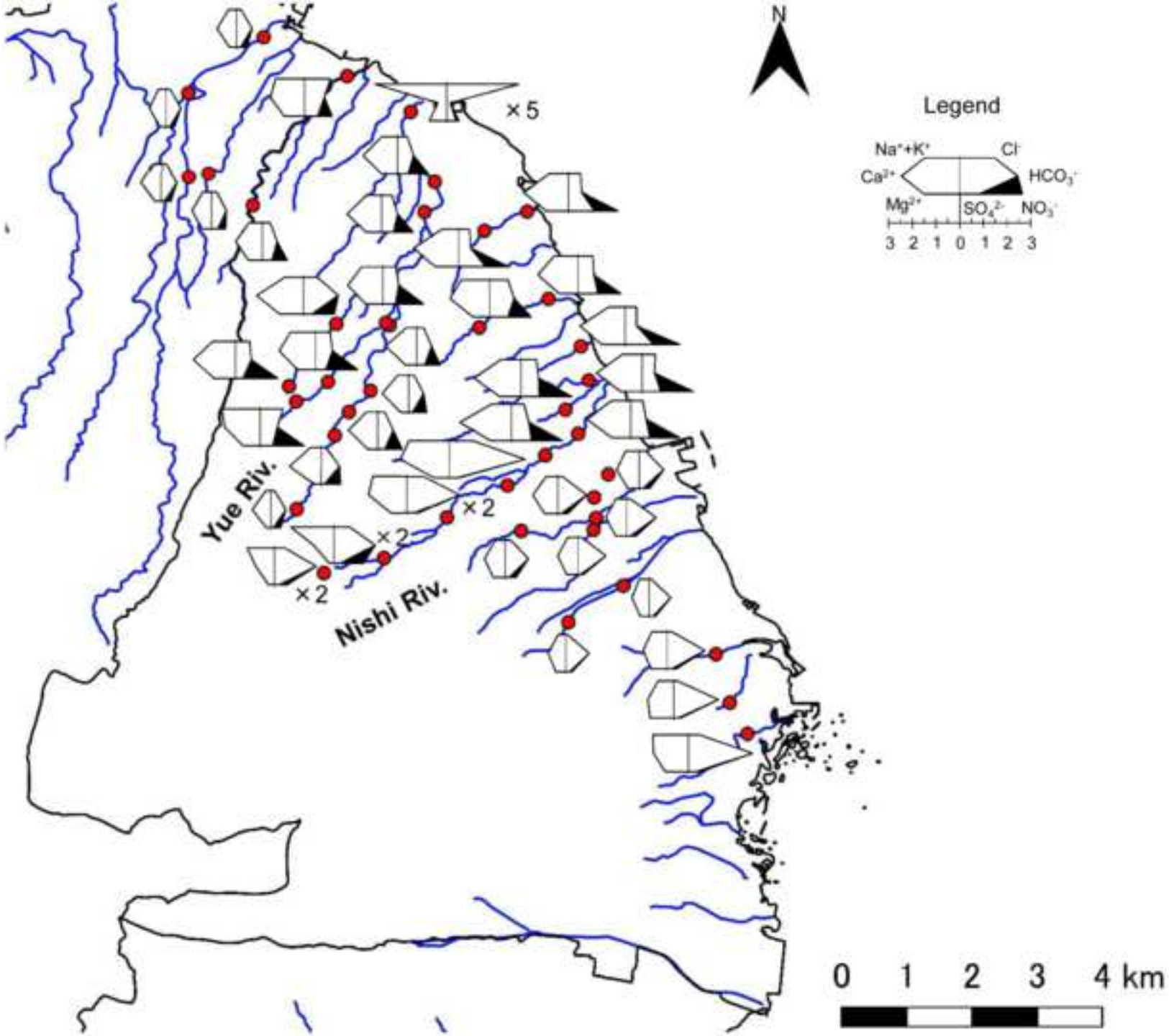

Figure 5

Click here to download Figure Fig 5.tif

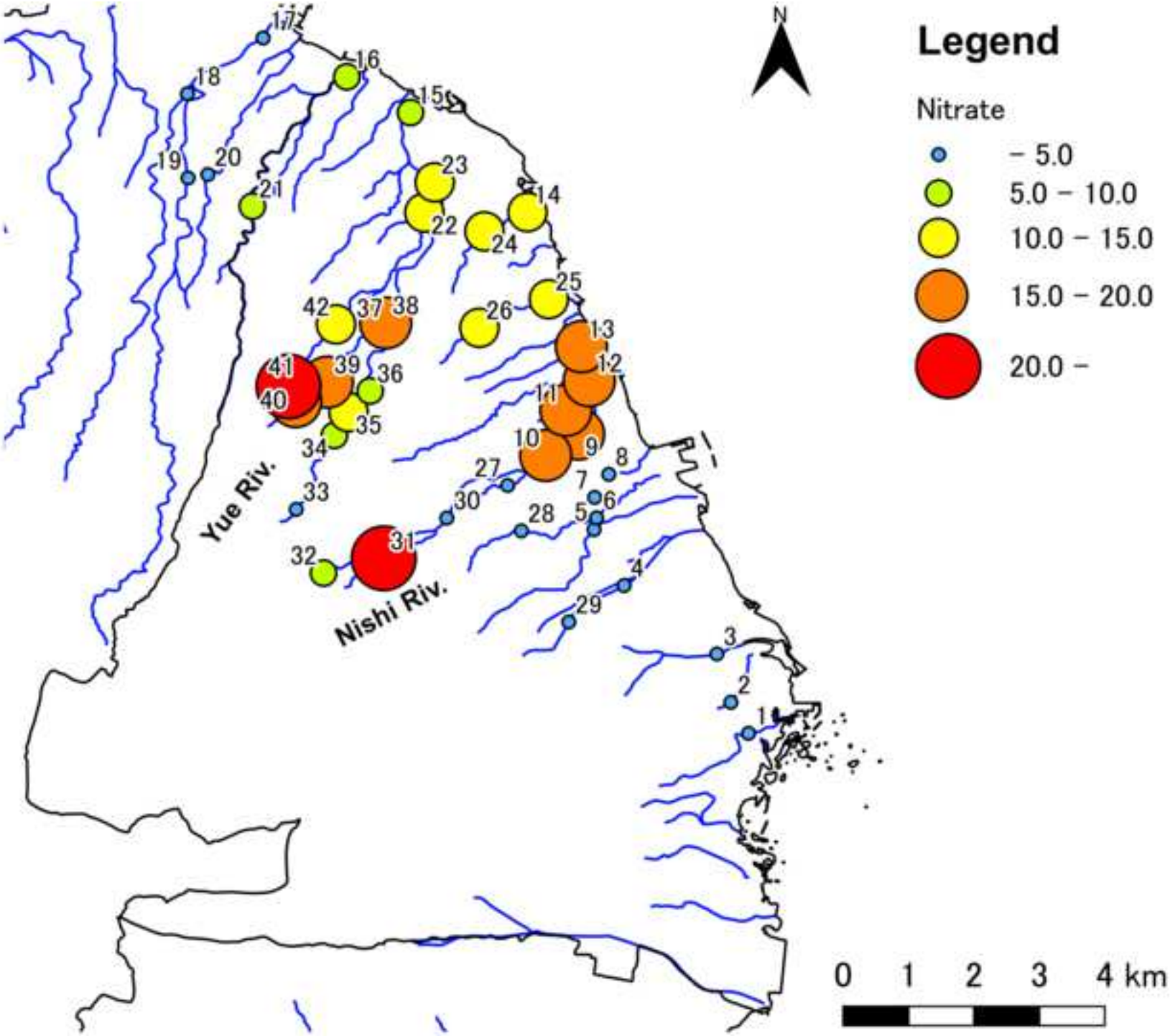

Figure 6

Click here to download Figure Fig 6.tif

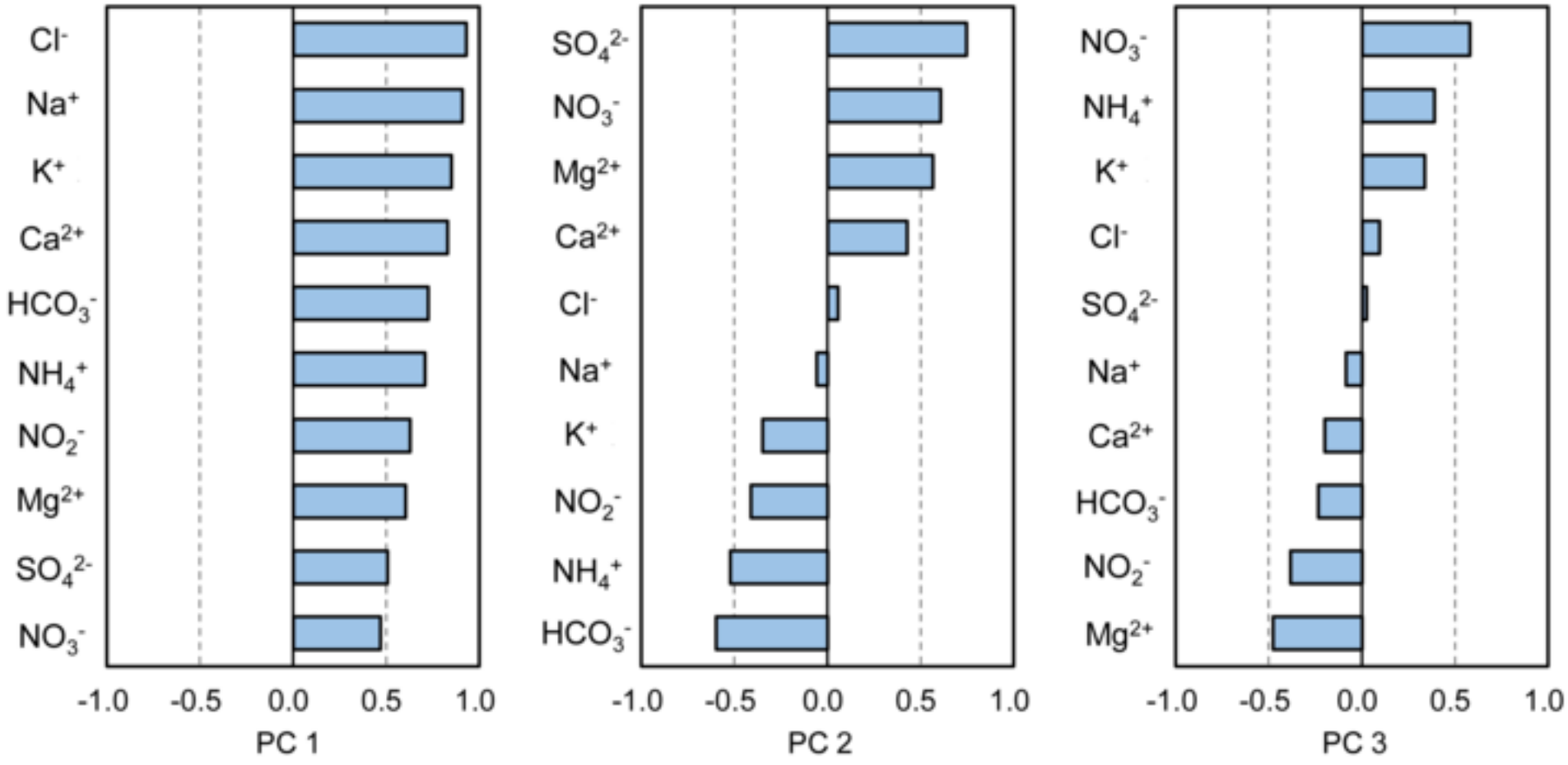

Figure 7

Click here to download Figure Fig 7.tif

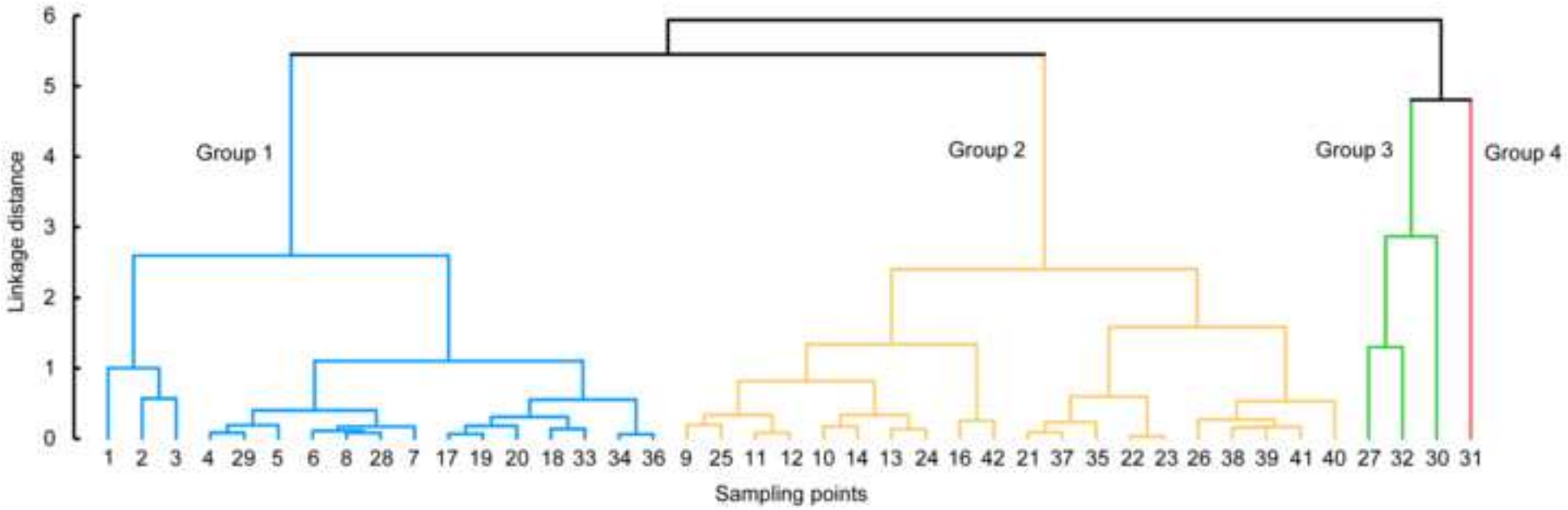

Figure 8

Click here to download Figure Fig 8.tif

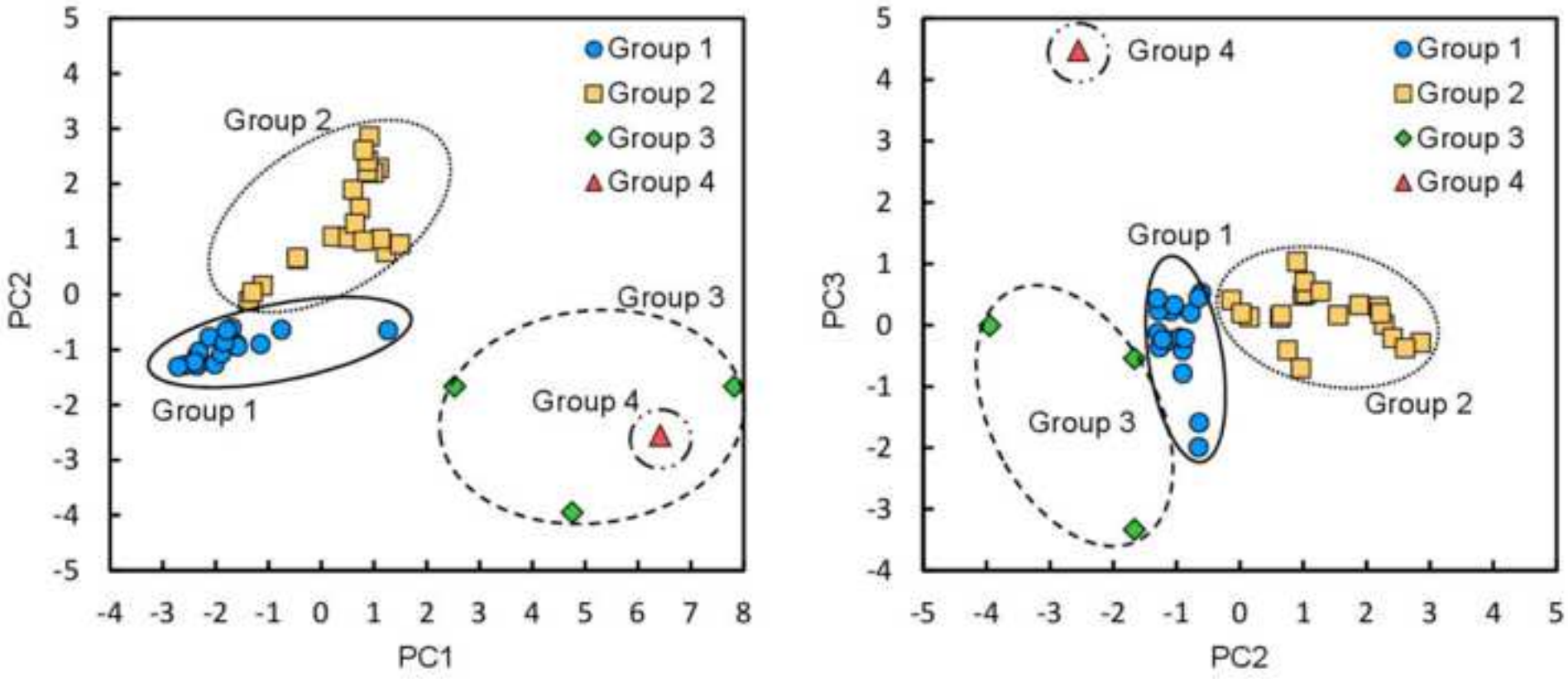

Figure 9

Click here to download Figure Fig 9.tif

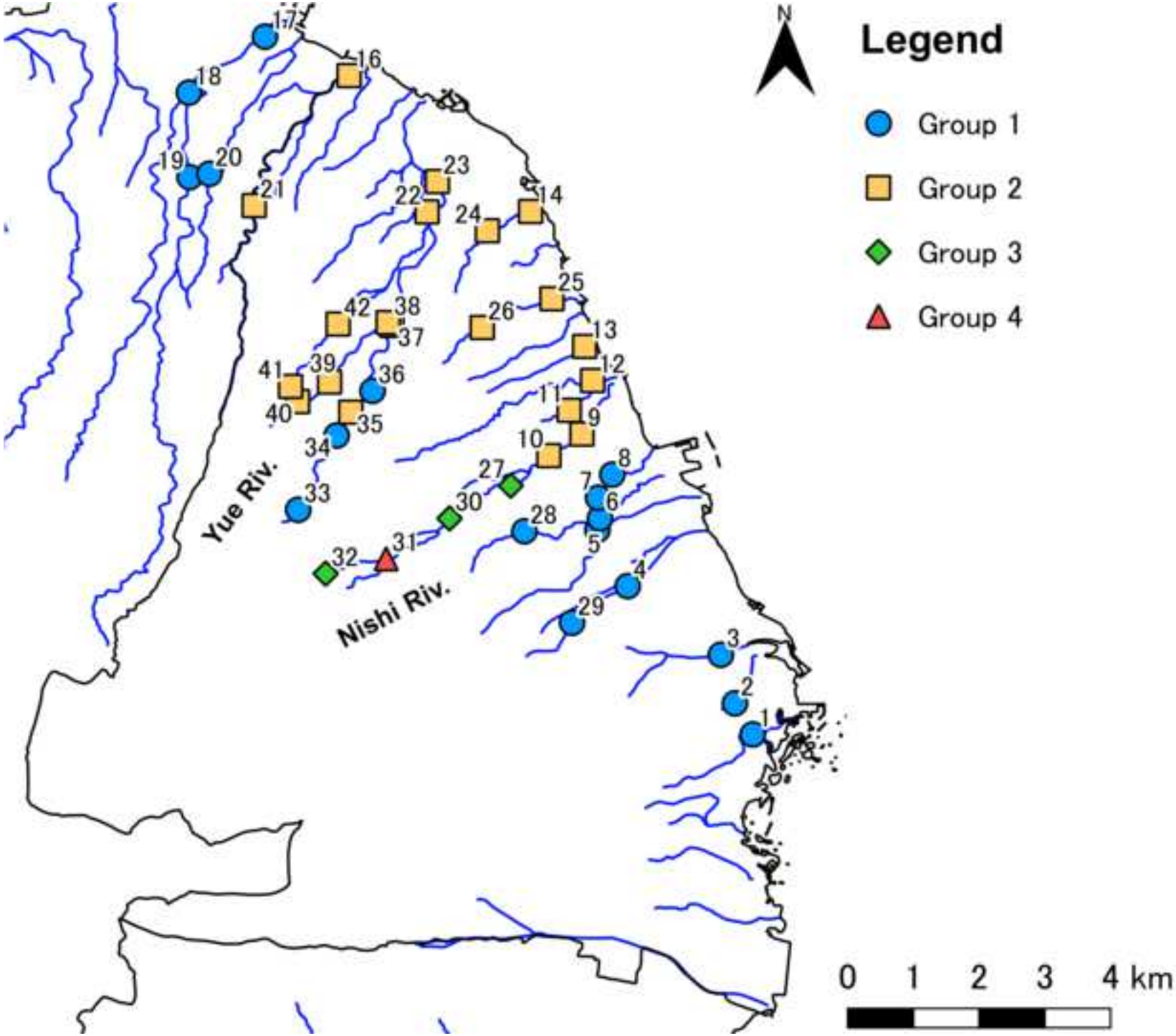

Table 1 Summary of measured hydrochemical parameters

site ID	Cl^- mg L^{-1}	NO_3^- mg L^{-1}	SO_4^{2-} mg L^{-1}	HCO_3^- mg L^{-1}	NO_2^- mg L^{-1}	Na^+ mg L^{-1}	K^+ mg L^{-1}	Mg^{2+} mg L^{-1}	Ca^{2+} mg L^{-1}	NH_4^+ mg L^{-1}	pH	EC mS m^{-1}	ORP mV	DO mg L^{-1}	Temp. ℃
1	16.6	8.5	14.4	167.2	N. D.	32.7	4.2	12.2	30.2	N. D.	6.12	38.6	171	10.88	17.2
2	6.0	6.3	9.3	117.5	N. D.	13.6	3.6	12.2	22.0	N. D.	7.04	24.4	268	10.63	14.1
3	7.7	12.1	10.4	99.8	N. D.	12.0	5.2	8.4	20.6	N. D.	7.05	23.8	280	11.22	15.9
4	3.7	5.6	9.0	56.7	N. D.	7.5	3.3	4.6	14.8	N. D.	6.61	14.64	147	11.50	13.9
5	5.6	7.5	5.6	72.9	N. D.	7.8	3.9	5.9	17.6	N. D.	6.78	16.97	240	10.89	15.7
6	5.6	14.7	7.4	68.6	N. D.	8.8	4.0	5.9	18.2	N. D.	6.29	21.0	240	10.88	16.4
7	7.4	16.0	7.9	76.0	N. D.	8.6	4.3	6.9	21.1	N. D.	6.44	19.70	257	10.68	14.7
8	9.8	17.1	8.3	64.4	N. D.	10.8	4.2	6.0	19.5	N. D.	6.51	20.2	208	11.09	11.8
9	18.4	80.2	39.7	40.9	N. D.	14.3	7.4	9.7	37.4	N. D.	6.50	35.5	179	10.99	13.7
10	19.0	80.4	42.2	45.8	N. D.	14.6	8.5	11.1	44.7	N. D.	6.73	41.6	240	11.15	11.9
11	23.6	87.4	37.7	32.3	N. D.	15.1	7.8	10.9	40.1	N. D.	6.94	42.4	246	10.15	12.5
12	19.7	85.5	38.5	30.8	N. D.	15.5	7.4	11.3	39.3	N. D.	7.00	46.3	257	10.89	12.6
13	16.8	69.0	59.4	29.9	N. D.	14.3	4.1	12.3	39.3	N. D.	6.97	41.1	253	11.28	12.1
14	19.1	63.3	53.7	35.1	N. D.	14.7	6.6	11.4	38.7	N. D.	6.71	36.1	265	10.42	14.3
15	547.1	38.8	93.2	47.0	N. D.	330.1	44.4	46.6	41.2	N. D.	6.68	205.0	210	11.04	14.4
16	39.7	38.7	27.4	53.1	N. D.	24.9	5.7	10.3	28.9	N. D.	6.65	53.0	239	11.23	14.9
17	7.1	15.4	9.3	40.9	N. D.	6.8	2.1	3.6	16.7	N. D.	6.57	19.60	239	11.08	8.7
18	6.7	12.3	8.0	38.1	N. D.	6.2	1.8	3.4	14.4	N. D.	6.15	16.12	249	10.96	10.7
19	6.4	16.8	7.2	40.6	N. D.	6.4	2.9	3.2	17.2	N. D.	6.31	17.50	28.1	10.42	9.9
20	8.4	19.4	13.7	39.4	N. D.	7.1	2.7	4.6	16.4	N. D.	6.68	17.52	268	10.94	8.9
21	12.7	39.8	20.9	40.0	N. D.	10.0	4.4	7.2	23.0	N. D.	6.59	23.8	263	10.88	13

22	15.4	52.3	23.2	42.1	N. D.	11.6	6.9	8.3	29.4	N. D.	6.48	26.8	223	10.98	12.5
23	15.8	52.6	24.3	42.1	N. D.	11.3	6.7	8.1	29.4	N. D.	6.69	29.3	216	11.58	11
24	16.6	61.1	56.7	31.7	N. D.	14.0	5.2	12.1	38.9	N. D.	6.74	35.9	246	11.15	11.4
25	22.2	61.7	40.7	41.5	N. D.	15.1	14.0	9.8	34.7	N. D.	6.66	40.6	239	10.95	10.6
26	27.7	60.8	38.2	64.4	N. D.	15.7	20.9	8.6	34.0	2.4	6.69	46.0	259	9.61	9.3
27	36.7	4.5	16.9	198.0	N. D.	21.8	30.6	7.9	42.0	12.3	6.75	65.0	26.5	7.82	4.9
28	8.2	17.8	7.9	60.1	N. D.	7.6	3.8	6.6	18.2	N. D.	6.93	19.0	248	10.72	11.5
29	2.5	6.9	7.8	60.7	N. D.	6.1	2.5	5.3	15.4	N. D.	7.00	14.6	249	10.89	8.8
30	52.3	20.1	31.9	275.2	12.0	33.1	57.0	16.3	65.5	14.9	6.12	78.6	205	2.48	10.5
31	47.4	121.6	25.3	214.8	N. D.	32.6	90.3	5.4	35.0	47.6	6.02	113.2	180	0.70	7.4
32	31.9	38.1	20.0	216.6	10.6	25.3	47.4	6.4	32.0	36.2	5.95	72.3	211	1.51	9.4
33	4.9	18.2	4.5	38.1	N. D.	4.7	1.4	2.6	16.1	N. D.	6.10	14.76	233	10.55	9.7
34	7.5	41.5	7.9	47.9	N. D.	7.4	4.9	3.6	27.1	N. D.	6.41	30.60	242	11.27	13.1
35	10.5	45.9	13.9	39.7	N. D.	9.5	3.2	5.3	25.4	N. D.	6.46	18.20	244	11.27	13.9
36	8.8	37.5	7.5	39.7	N. D.	8.9	3.2	4.2	22.5	N. D.	6.30	23.8	253	11.00	15.3
37	10.5	41.3	16.5	39.4	N. D.	9.4	1.7	6.0	26.9	N. D.	6.11	37.0	247	10.87	14.8
38	20.2	74.4	25.5	41.8	N. D.	13.7	12.7	9.2	30.2	N. D.	6.13	34.6	246	10.78	12.7
39	22.8	84.9	21.7	44.8	N. D.	15.7	14.8	9.2	31.0	N. D.	6.03	47.9	247	10.83	13.5
40	34.1	83.4	25.3	44.8	N. D.	20.7	29.6	8.9	30.7	N. D.	6.12	60.5	249	10.25	12.7
41	22.4	92.0	16.4	42.7	N. D.	13.2	15.6	10.9	35.8	N. D.	6.28	43.2	248	10.79	11.6
42	20.9	59.8	16.7	90.0	N. D.	14.3	7.2	12.6	40.1	N. D.	6.40	34.6	220	10.84	13.7

Table 2 Correlation matrix between dissolved ions

	NO_3^-	SO_4^{2-}	HCO_3^-	NO_2^-	Na^+	K^+	Mg^{2+}	Ca^{2+}	NH_4^+
Cl^-	0.50**	0.47**	0.59**	0.49**	0.87**	0.81**	0.52**	0.77**	0.60**
NO_3^-		0.64**	-0.17	-0.11	0.32*	0.38*	0.37*	0.55**	0.24
SO_4^{2-}			-0.10	0.07	0.37*	0.18	0.66**	0.71**	0.05
HCO_3^-				0.69**	0.74**	0.76**	0.25	0.40**	0.75**
NO_2^-					0.49**	0.54**	0.26	0.45**	0.53**
Na^+						0.74**	0.59**	0.67**	0.61**
K^+							0.17	0.50**	0.90**
Mg^{2+}								0.80**	-0.05
Ca^{2+}									0.28

* Correlations significant at $p = 0.05$

** Correlations significant at $p = 0.01$

$n = 41$ (except for site 15 where the water is mixed with sea water)

Table 3 Averaged dissolved ion concentrations for each groups

	samples	Cl^- mg L^{-1}	NO_3^- mg L^{-1}	SO_4^{2-} mg L^{-1}	HCO_3^- mg L^{-1}	NO_2^- mg L^{-1}	Na^+ mg L^{-1}	K^+ mg L^{-1}	Mg^{2+} mg L^{-1}	Ca^{2+} mg L^{-1}	NH_4^+ mg L^{-1}
Group 1	17	7.3	16.1	8.7	66.4	0.1	9.6	3.4	5.8	19.3	0.2
Group 2	20	20.4	65.7	31.9	43.6	0.1	14.4	9.5	9.6	33.9	0.3
Group 3	3	40.3	20.9	22.9	229.9	7.6	26.7	45.0	10.2	46.5	21.1
Group 4	1	47.4	121.6	25.3	214.8	0.1	32.6	90.3	5.4	35.0	47.6